REPORT ON
EDDY CURRENT SEPARATORS

Prepared for

Mr John Curwen
Eriez Magnetics Europe Ltd

Project Number 10866 – 367

4th January 2013

Prepared By Iain S Wells, BSc., Ph.D., C. Eng.

Magnetic & Electrostatic Specialist, Metallurgical Operations, UK

Authorised By N.J. MacDonald, BSc, EngTech, TIMMM

Operations Manager, European Metallurgical Operations

NOTE:
This report refers to the samples as received.

Disclaimer

Executive Summary

In this study into the relative performance of three different Eddy Current Separators, two produced by Eriez Magnetics Europe and one purchased through a third party from Steinert of Germany, has been explored. The basic parameters of each unit were measured and then each was subjected to a comprehensive series of tests to compare the performance. A total of six different non-ferrous test pieces were tested at different rotor and belt speeds on each of the machines.

In order to make direct comparisons, each of the units was installed and set up so that the test pieces could be collected in a purpose built tray, so that the deflection from a datum point could be measured. To establish the actual nett deflection imparted by the eddy current separator the deflection of non-metallic particles of similar size and mass were also measured. The gross throw, as well as the nett deflection was then plotted for each type of test piece against the rate of pole reversal (Hz), for each of the machines so that it could be ascertained which of the units produced the longest throw and deflection.

The results demonstrate that, for the types of non-ferrous metals selected and the parameters explored, the Eriez ST-22-C performs best overall, by producing a greater throw and deflection for the majority of materials. The increase in throw and deflection was found to be up to 200mm more than the Steinert unit tested. The exceptions were for large fragmentised aluminium scrap upon which the Eriez ST-2-C produced the best results. However, the Steinert NES 50 120 produced a slightly longer throw and deflection with the small round and flat aluminium particles at the lower of the two belt speeds trialled, but at the higher belt speed the Eriez ST-22-C delivered a longer throw and deflection than the Steinert unit.

Table of Contents

Table of Tables

Table of Figures

1. Introduction

Eriez Magnetics Europe Ltd. (Eriez), part of Eriez Magnetics International, manufactures a range of Eddy Current Separators (ECS) that are supplied into the recycling industry for a variety of applications. Whilst Eriez Magnetics supply a significant number of ECS units worldwide they encounter Steinert Elektromagnetbau GmbH (Steinert), based in Germany, as a competitor.

Eriez have themselves developed a number of different ECS of varying designs, suitable for different applications that have been recently evaluated by a team of their own engineers. As part of this programme, Eriez has acquired a Model NES 50 120 unit, manufactured by Steinert, on which comparative tests have also been carried out. These tests have utilised both regular shapes and typical items of non-ferrous metal pieces, to determine the displacement imparted to the objects by the various ECS machines. SGS Minerals Services have been requested by Eriez to conduct an independent test programme to evaluate the relative performance of two types of Eriez ECS as well as that of Steinert. It is Eriez's intention to publish or quote from the independent report for marketing purposes.

1.1 Background

1.1.1 History of Discovery of Eddy Currents

The first person to observe current eddies was François Arago In 1824, the 25th Prime Minister of France, who was also a mathematician, physicist and astronomer. He observed what he termed "rotatory" magnetism, and the fact that most conductive bodies could be magnetized; these discoveries being completed and explained by Michael Faraday.

In 1834, Heinrich Lenz stated Lenz's law, which says that the direction of induced current flow in an object will be such that its magnetic field will oppose the magnetic field that caused the current flow. Eddy currents develop secondary flux that cancels a part of the external flux.

French physicist Léon Foucault is credited with having discovered Eddy currents in September, 1855 when he discovered that the force required for the rotation of a copper disc becomes greater when it is made to rotate with its rim between the poles of a magnet, the disc at the same time becoming heated by the eddy current induced in the metal.

1.1.2 Explanation of Eddy Currents

Eddy currents (also called Foucault currents) are electric currents induced in conductors when a conductor is exposed to a changing magnetic field; due to relative motion of the field source and conductor or due to variations of the field with time. This can cause a circulating flow of electrons, or current, within the body of the conductor. These circulating eddies of current have inductance and thus induce magnetic fields. These fields can cause repulsive, attractive, propulsion and drag effects. The stronger the applied magnetic field, or the greater the electrical conductivity of the conductor, or the faster the field changes, then the greater the currents that are developed and the greater the fields produced.

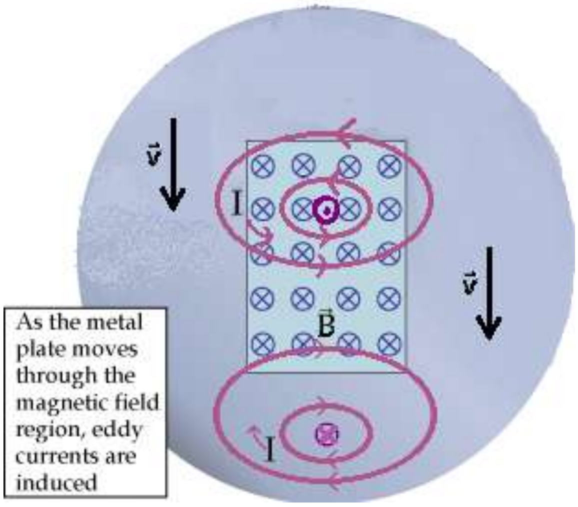

Figure 1 Diagram Illustrating the Formation of Eddy Currents When a Metal Plate Passes Through a Magnetic Field

Eddy currents, like all electric currents, generate heat as well as electromagnetic forces. The heat can be harnessed for induction heating. The electromagnetic forces can be used for levitation, creating movement, or to give a strong braking effect. Eddy currents can also have undesirable effects, for instance power loss in transformers. In this latter application, they are minimised with thin plates, by lamination of conductors or by adapting other details of the conductor shape.

Self-induced eddy currents are responsible for the skin effect in conductors. The latter can be used for non-destructive testing of materials for geometry features, like micro-cracks. A similar effect is the proximity effect, which is caused by externally-induced eddy currents.

References:

- Fitzgerald, A. E.; Kingsley, Charles Jr. and Umans, Stephen D. (1983). *Electric Machinery* (4th ed.). Mc-Graw-Hill, Inc.. pp. 20. ISBN 0-07-021145-0.
- Sears, Francis Weston; Zemansky, Mark W. (1955). *University Physics* (2nd ed.). Addison-Wesley. pp. 616–618.

1.2 Principle of Operation of Eddy Current Separators

Eddy Current Separators, also known as Non-ferrous Metal Separators, consist of a short conveyor that delivers the material to be separated to the head drum. A rapidly rotating system of permanent magnets is incorporated into this head drum, which generates high-frequency changing magnetic fields. These high frequency fields create strong eddy currents within the non-ferrous metal particles. These eddy currents circulating within the non-ferrous particles generate their own internal magnetic fields that oppose the externally applied high frequency field. As both magnetic fields are of the same polarity repulsion occurs and the non-ferrous particle is thrown or flipped from the head drum as illustrated in Figure 2 below.

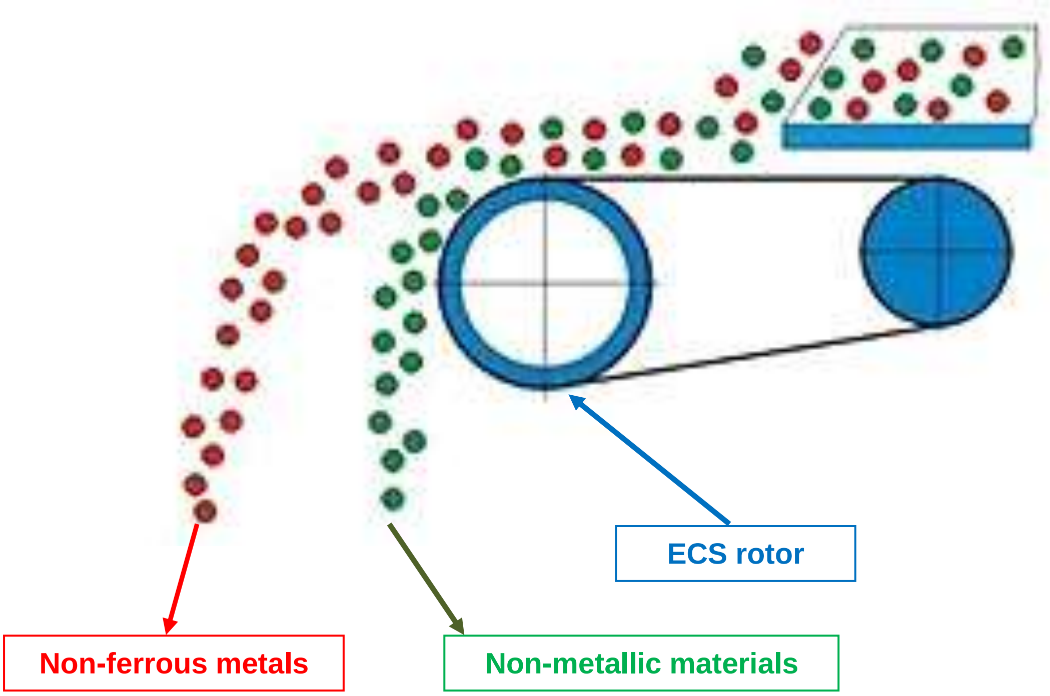

Figure 2 Diagram of Operation of ECS

1.3 Objectives

The principal objective of this programme of tests on Eddy Current Separators was as follows;

- To conduct a comparative study of two ECS machines produced by Eriez, i.e. Models ST-22-C and ST-2-C with a Model NES 50 120 produced by Steinert

2 Parameters of the ECS Machines Investigated

The basic mechanical and magnetic parameters were measured and verified as tabulated below in Table 1.

Table 1 Parameters of the Three ECS Machines Tested

ECS Model	Rotor dia, mm	External shell dia. mm	No. of poles	Rotor speed range, rpm	Frequency range, Hz	Belt thickness, mm	Magnet block dimensions. L x W x H mm
Eriez ST-22-C	205	414	22	0 – 4,500	0 – 825	2	25.4 x 43.1 x 20
Eriez ST-2-C	205	414	14	0 – 4,500	0 - 525	2	50.8 x 43.1 x 20
Steinert NES 50 120	406	610	38	600 - 2593	190 – 821.1	2	34 long by 20 thick

There are some immediate and obvious differences in the basic parameters of the machines that are summarised as follows.

- The diameter of the Steinert rotor is significantly larger than the Eriez units (610mm cf. 414mm).
- Whilst the Steinert machine has a greater number of magnet poles (38 cf. 22 for the Eriez ST-22-C) a significantly higher frequency is attained by the ST-22-C, which will assist in maximising the eddy current forces, as its maximum operating rotational speed is higher (4,500 cf. 2,593 rpm).
- The Steinert machine (Figure 7) was the most compact of the three. The position of the eccentric rotor of the Steinert unit was easily adjusted (Figure 8) without any tools, whereas for the Eriez units spanners were required. The visual indication of the position of the Steinert eccentric rotor was more apparent than either of the Eriez units.
- The Steinert unit is of a high engineering standard with machined magnet carrier drums and consequently a precision fit on the end flanges.
- The Eriez ST-22-C and ST-2-C are fitted with a shell constructed of high technology material to minimise the distance between the rotor and belt surface to maximise the effectiveness of the magnetic forces produced (Figure 5).

- The minimum speed for the Steinert unit was 600 and the maximum 2593 rpm whilst for the Eriez Models ST-22-C and ST-2-C the corresponding figures were 0 and 4,500 respectively.
- It is not possible to turn the rotor of the Steinert unit off without also turning off the belt.

Figure 4 Eriez ECS Model ST-22-C with Guards Removed

Figure 3 Eriez ECS Model ST-2-C with Guards Removed

Figure 5 Eriez ST-22-C Fitted with a High Technology Material Shell

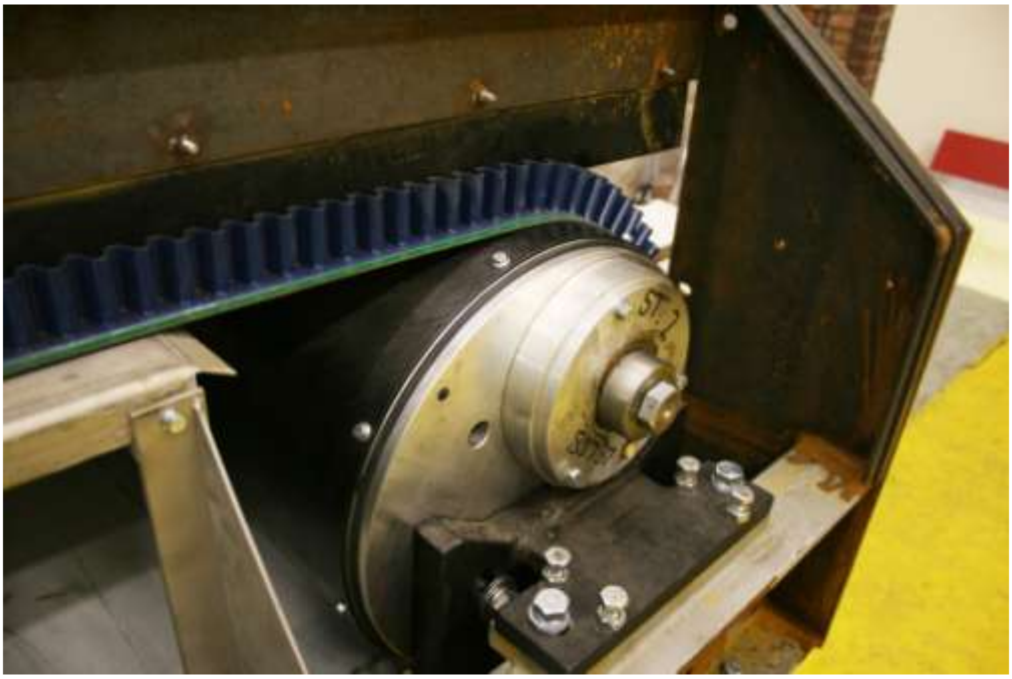

Figure 6 Eriez ST-2-C Showing Rotor in 22° Position

Figure 7 ECS Manufactured by Steinert

Figure 8 Detail of Steinert Eccentric Rotor Adjustment Mechanism in the 22° Position

3 Design of Test Programme

The tests were carried out independently by SGS Minerals Services personnel at the premises of Eriez Magnetics Europe Ltd (Eriez) in Caerphilly, Wales. Eriez provided assistance, equipment etc. as requested by SGS.

It was evident from the initial investigation of the basic parameters of the three machines that were to be investigated that there were detail differences in their dimensions as well as internal magnetic structures (rotor). For the purposes of this investigation it was decided to utilise 6 different types of non-ferrous metal in order to achieve as comprehensive review of the respective performances as possible. The properties of the materials selected have been tabulated in Table 2.

Table 2 Properties of Materials Selected for Testing

Material description	*No. of test pieces*	*Approximate size in mm*	*Average mass, g*
Small fragmentised aluminium	25	- 20 + 5	1.2
Large fragmentised aluminium	13	- 100 + 25	22.0
Copper test pieces	5	15 by 17 by 3	7.5
Aluminium test pieces	4	17 by 17 by 3	2.4
Round aluminium pieces	18	5 – 6mm diameter	0.24
Flat aluminium pieces	18	5 – 6	0.04

For the purposes of this investigation the term “throw” was defined as the distance travelled by the piece(s) under investigation from a datum point defined as the top dead centre of the head drum as shown in the accompanying diagram, Figure 10. Deflection was defined as the difference between the throw of a non-ferrous test material and that of an equivalent size/mass non-metallic control piece (see Table 6 for details).

The particles were caught in a purpose built Perspex catch-tray filled with dry glass sand, to reduce the incidence of bouncing. If a particle bounced it was possible to ascertain the original point of contact from the impression left in the sand. This tray is illustrated in Figure 9.

It was evident from initial trials that the throw of the individual particles would be subject to a degree of scatter due to the large number of variables involved. Consequently a number of test pieces were tested as indicated above in Table 2.

Figure 9 Perspex Catch-Tray Filled with Glass Sand to Catch the Test Pieces Deflected by the ECS

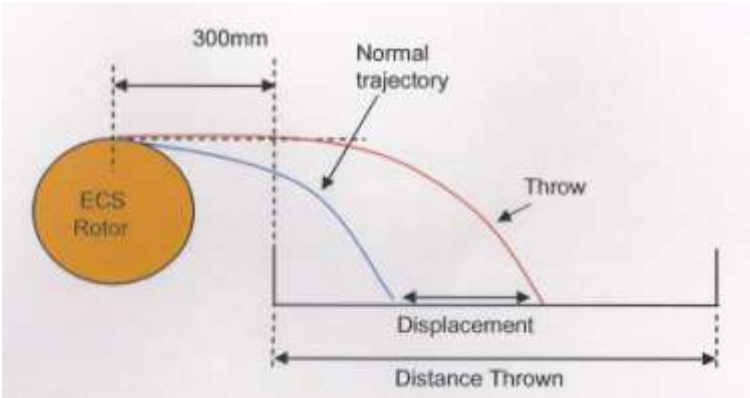

Figure 10 Diagram Showing the Position of the Catch-Tray Relative to the ECS Rotor

For each type of material and each of the three machines two different belt speeds were deployed in parallel tests, one at 102 m/min and the other at 144 m/min, which was measured by means of a tachometer. The speed of the ECS rotors was measured on the drive shaft also by means of a tachometer; the speeds used for each of the three machines are tabulated for the pre-selected rotor speeds in Tables 3 through 5 below.

Table 3 Eriez Model ST-22-C Frequency of Pole Reversals

ECS Model Eriez ST-22-C		
Rotor speed rpm	No. of poles	Pole reversals, Hz
2000	22	366.7
2500		458.3
3000		550.0

Table 4 Eriez Model ST-2-C Frequency of Pole Reversals

ECS Model Eriez ST-2-C		
Rotor speed rpm	No. of poles	Pole reversals, Hz
2000	14	233.3
2500		291.7
3000		350.0

Table 5 Steinert Frequency of Pole Reversals

ECS Steinert Model *NES 50 120*		
Rotor speed rpm	No. of poles	Pole reversals, Hz
1000	38	316.7
1500		475.0
2000		633.3
2593		821.1

The control pieces were used to ascertain the ballistic trajectory of a particle of similar weight, shape and size as the non-ferrous test pieces to determine the net deflection are tabulated in Table 6 below.

Table 6 Details of Non-Metallic Test Pieces used to Establish the Net Deflection of the Non-Ferrous Test Pieces

Material description	*Non-metallic test piece*	*Approximate size in mm*	*Average mass, g*
Small fragmentised aluminium	Stone and plastic	- 20 + 5	2.3, 0.9
Large fragmentised aluminium	Stone and wood	~25	97.9, 47.9
Copper test pieces	Wood and plastic squares	17 by 17 by 3	0.75, 0.47
Aluminium test pieces	Wood and plastic squares	17 by 17 by 3	0.75, 0.47
Round aluminium pieces	Plastic	5 – 6mm diameter	0.05
Flat aluminium pieces	Plastic	5 – 6	0.05

The various non-metallic test pieces selected are illustrated in Figures11 through 14.

Figure 11 Stone and Plastic Non-Metallic Test Pieces

Figure 12 Large Piece of Wood used as a Non-Metallic Test Piece

Figure 13 Large Piece of Stone used as a Non-Metallic Test Piece

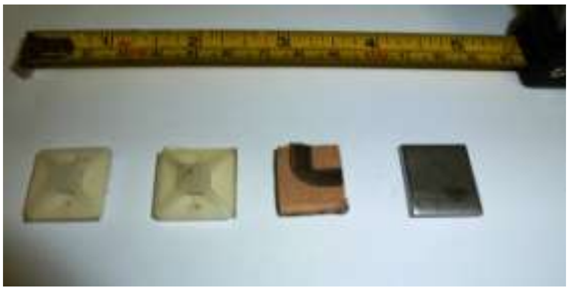

Figure 14 Flat Pieces of Plastic, Card and Non-Ferrous Metal used as Non-Metallic Test Pieces

Each of the three ECS units were set-up in accordance with the manufacturers instructions with the rotor running forwards (for the Eriez and Steinert units it is also possible to reverse the direction of the rotation of the rotor) and the position of the rotor relative to the vertical of 22° for the Steinert and Eriez ST-22-C. However, it had been initially observed in preliminary trials with the Eriez Model ST-2-C that superior results were achieved with the rotor in a vertical position and so consequently the tests were conducted with the rotor in this position.

4 Comparative ECS Test Programme

For each run with a specific test piece the items were carefully placed onto the moving transport belt, avoiding the cleat, at a speed of 102 then 144 m/min at the pre-selected rotor speeds. The test items were placed individually so that they could not interfere without each other, towards the centre line of the belt, to avoid any potential edge effects and for consistency. The positions where the individual items fell initially into the glass sand was measured from the datum point and the results recorded. If the spread of results was too large then the test was repeated. Similarly with any items that struck the catch-tray or missed the tray altogether the test was repeated.

Figure 15 Typical Disposition of Small Fragmentised Aluminium after Test

Figure 16 Flat Aluminium Particles in the Catch-Tray Showing Initial Impact Sites

Figure 17 Large Fragmentised Aluminium after Test

Figure 18 Catch-Tray in Position in front of Steinert ECS

5 Results and Observations on Test Programme

5.1.1 Small Fragmentised Aluminium

The throw for the small fragmentised aluminium is displayed graphically in Figure 19 and Figure 20.

It can be seen from the two graphs that the Eriez ST-22-C ECS delivers a throw of in excess of 200mm more than the Steinert machine at a belt speed of 144 m/min, and 100mm at a belt speed of 102 m/min. The difference in the net deflection (Figure 31 and Figure 32) is the same and therefore would potentially translate into the Eriez ST-22-C achieving a superior separation on this type of fragmentised aluminium scrap on an industrial scale.

5.1.2 Large Fragmentised Aluminium

The throw for the large fragmentised aluminium is displayed graphically in Figure 21 and Figure 22.

It can be seen from the two graphs that both the Eriez ST-22-C and Eriez ST-2-C ECS deliver a throw of almost 200mm more than the Steinert machine at a belt speed of 144 m/min, and 100mm at a belt speed of 102 m/min. The difference in the nett deflection (Figure 33 and Figure 34) is the same and therefore would potentially translate into the Eriez ST-22-C and Eriez ST-2-C achieving a superior separation on this type of fragmentised aluminium scrap on an industrial scale.

Note the apparent peak in the throw for a frequency of 583.3 Hz observed with the Eriez ST-2-C.

5.1.3 Copper Test Pieces

The throw for the copper test pieces is displayed graphically in Figure 23 and Figure 24.

It can be seen from the two graphs that both the Eriez ST-22-C and Eriez ST-2-C ECS deliver a greater throw than the Steinert machine at both belt speeds.

5.1.4 Aluminium Test Pieces

The throw for the aluminium test pieces is displayed graphically in Figure 25 and Figure 26.
It can be seen from the two graphs that both the Eriez ST-22-C and Eriez ST-2-C ECS deliver a greater throw than the Steinert machine at both belt speeds.

5.1.5 Round Shaped Aluminium

The throw for the round shaped aluminium is displayed graphically in Figure 27 and Figure 28.

The Eriez ST-22-C unit delivers a similar throw to the Steinert ECS at a belt speed of 102 m/min but at the higher belt speed of 144 m/min the throw is more than the Steinert machine. The throw achieved by the Eriez ST-2-C is significantly less than either of the other two units.

5.1.6 Flat Shaped Aluminium

The throw for the flat shaped aluminium is displayed graphically in Figure 29 and Figure 30.

The Eriez ST-22-C unit delivers a similar throw to the Steinert ECS at a belt speed of 102 m/min but at the higher belt speed of 144 m/min the throw is more than the Steinert machine. The throw achieved by the Eriez ST-2-C is significantly less than either of the other two units.

5.2 Overall Performance Comparison

In Table 7 below the results of the test programme are summarised for each of the different types of test pieces investigated. It can be seen that the overall performance of the Eriez ST-22-C is the best. However, for the round and flat aluminium pieces the Steinert unit is better at the lower belt speed but the Eriez ST-22-C at the higher belt speed.

Table 7 Summary of Performance of the Different ECS

Material description	*Approximate size in mm*	*Average mass, g*	*Unit(s)for best throw*	*Comments*
Small fragmentised aluminium	- 20 + 5	1.2	Eriez ST-22-C	
Large fragmentised aluminium	- 100 + 25	22.0	Eriez ST-2-C	
Copper test pieces	15 by 17 by 3	7.5	Eriez ST-22-C	
Aluminium test pieces	17 by 17 by 3	2.4	Eriez ST-22-C	
Round aluminium pieces	5 – 6mm diameter	0.24	Steinert/ Eriez ST-22-C	Depends upon belt speed
Flat aluminium pieces	5 – 6	0.04	Steinert/ Eriez ST-22-C	Depends upon belt speed

6 Conclusions

- The Eriez ST-22-C performs better than the Steinert unit on most of the different shapes and particle sizes tested. The exception being the smaller round and flat aluminium pieces where the Steinert delivered a slightly greater throw at the lower belt speed whereas at the higher belt speed the ST-22-C achieved a greater throw.
- The Eriez ST-2-C performs best on the large pieces of fragmentised aluminium but not as well as the other two units with the smaller (and lighter) smaller round and flat aluminium pieces. According to Eriez this unit has been specifically designed to process larger items of non-ferrous metals
- There is a clear relationship between the number of pole reversals that a non-ferrous particle is subjected to and the distance that it is thrown. This is evidenced by the straight lines obtained when plotting the results on a linear basis. The exception is for the Eriez ST-2-C where there appears to be a maximum throw achieved at a frequency of 291.7 Hz. However, as only three different frequencies were tested this observation would require confirmation by conducting tests at lower and higher frequency.
- Whilst it is evident from the theory behind eddy current separation that the number of pole reversals is important in determining the throw imparted to an object there are other factors involved such as the magnetic field strength of the magnets, the depth of the magnetic field, and the position of the magnets relative the material to be separated. These other factors assist in explaining why the Eriez units achieve a greater throw than the Steinert unit which has a greater number of magnet poles.
- Increasing the speed of the conveyor belt generally increases the throw proportionately as can be observed by reference to the graphs from Figure 31 to Figure 34.
- The orientation of the test pieces with respect to the head drum was not investigated.
- The effect of inter particle reaction on the deflection of particles was eliminated from influencing the outcome of the test programme by ensuring that single particles were fed to the ECS units..

APPENDIX I

Graphs of the throw and deflection of various items of non-ferrous metals for the different ECS units

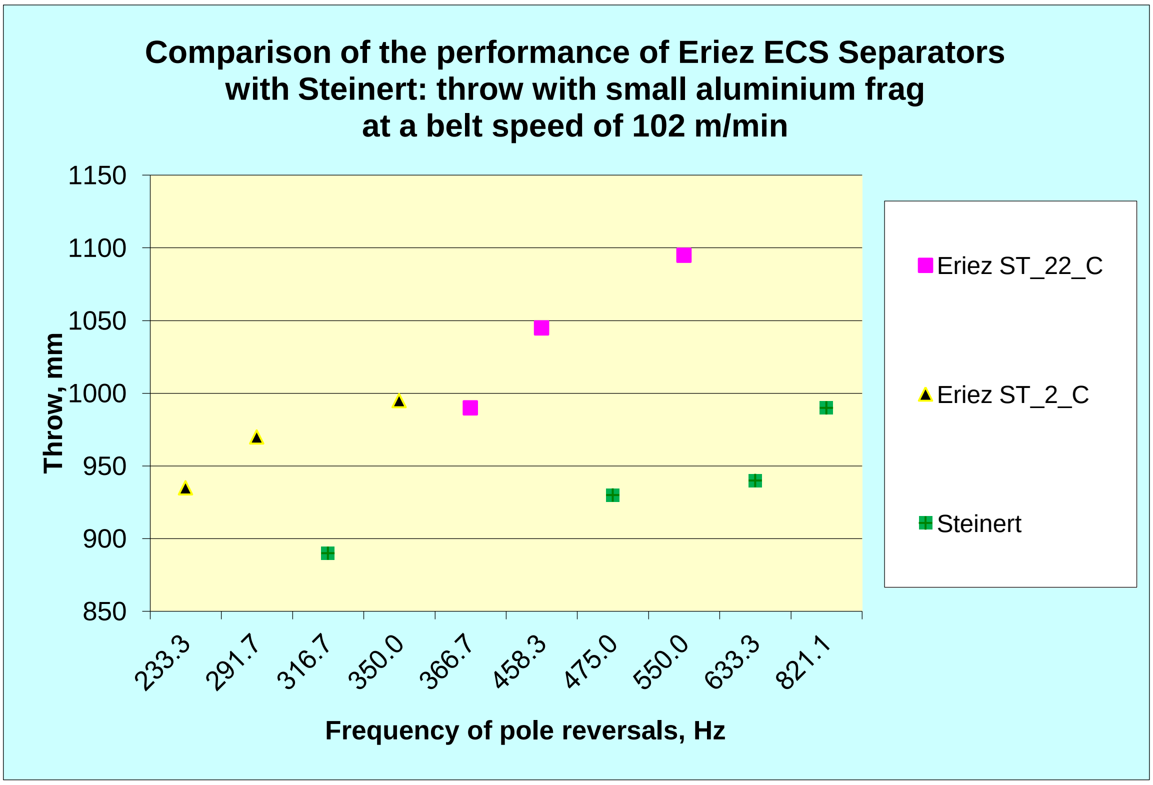

Figure 19 The Gross Throw of Small Particles of Fragmentised Aluminium at a Belt Speed of 102 m/min

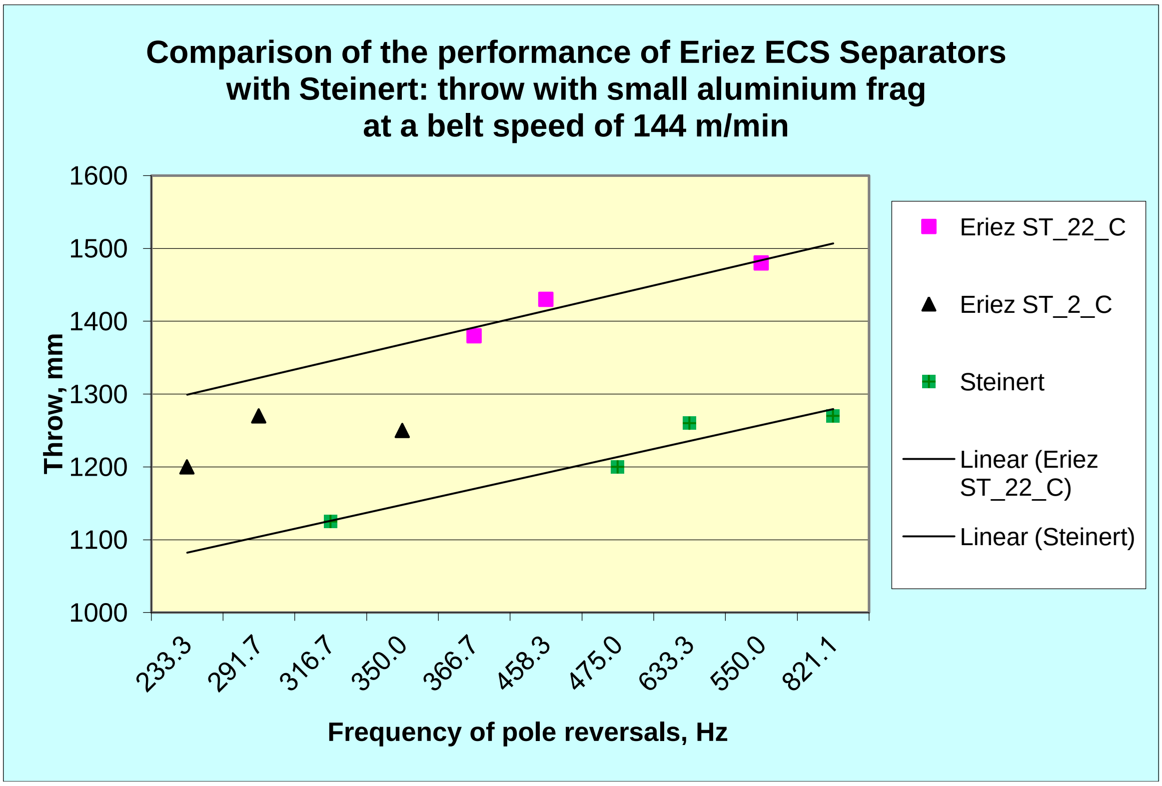

Figure 20 The Gross Throw of Small Particles of Fragmentised Aluminium at a Belt Speed of 144 m/min

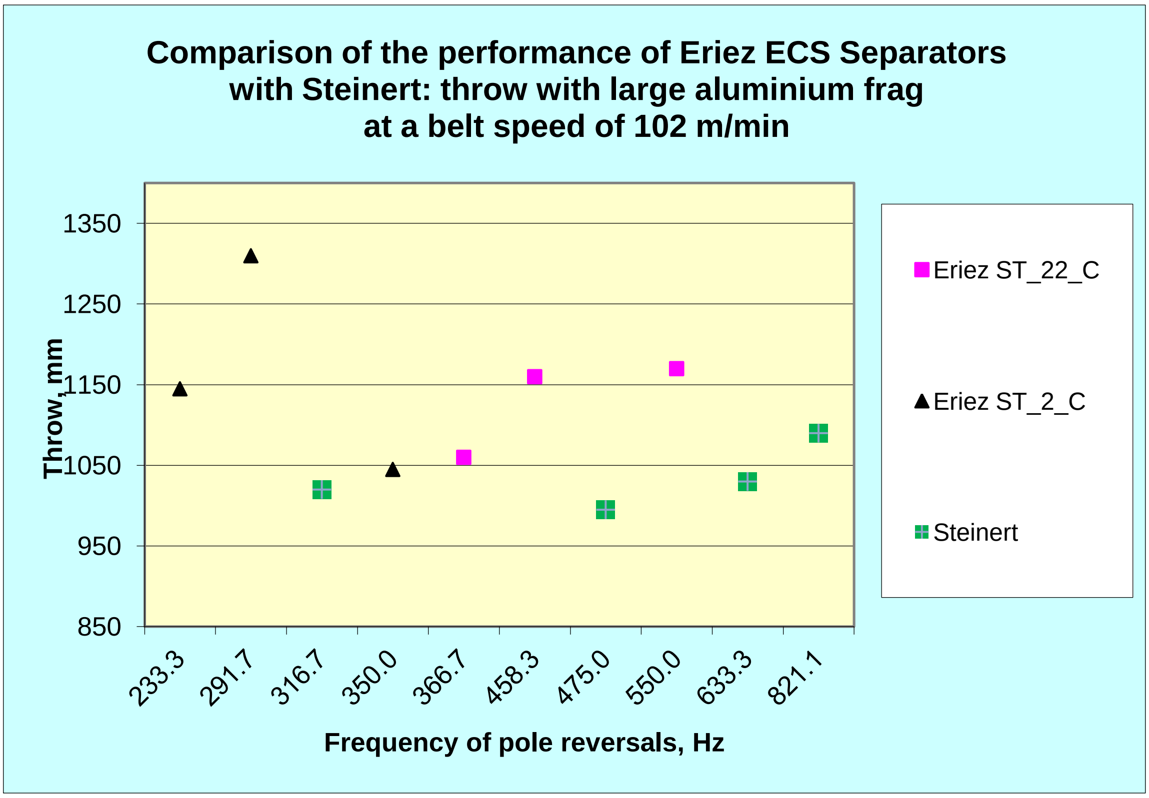

Figure 21 The Gross Throw of Large Particles of Fragmentised Aluminium at a Belt Speed of 102 m/min

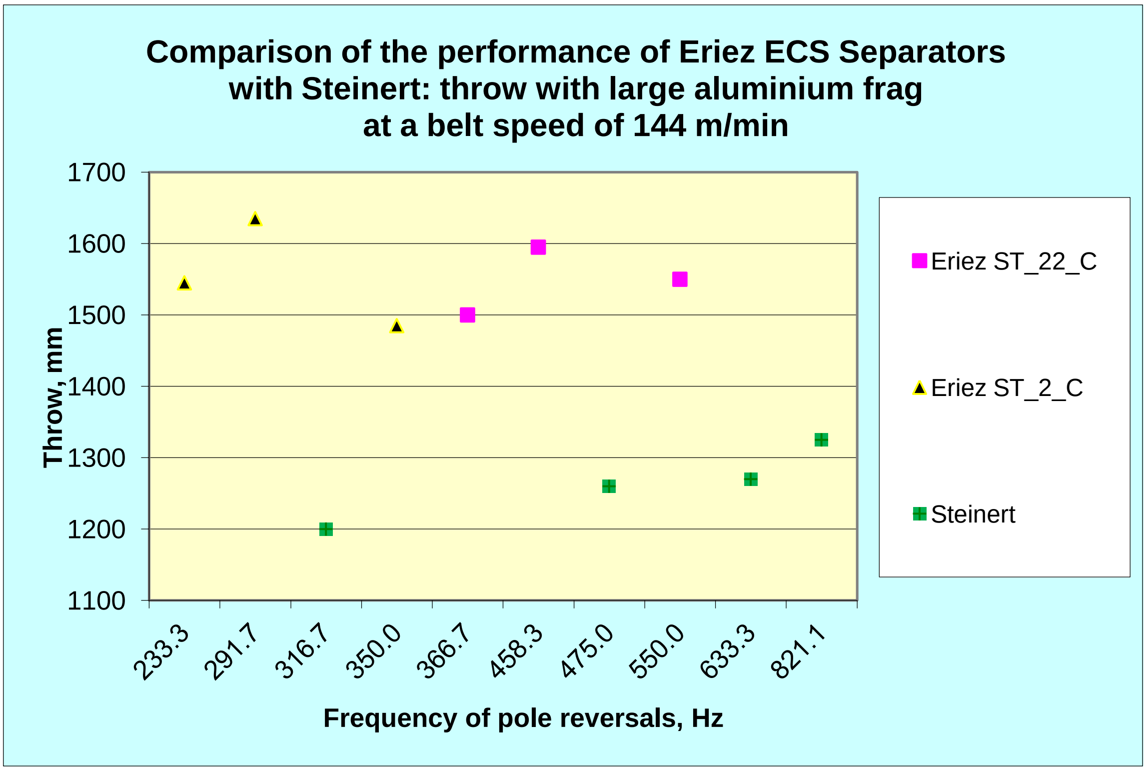

Figure 22 The Gross Throw of Large Particles of Fragmentised Aluminium at a Belt Speed of 144 m/min

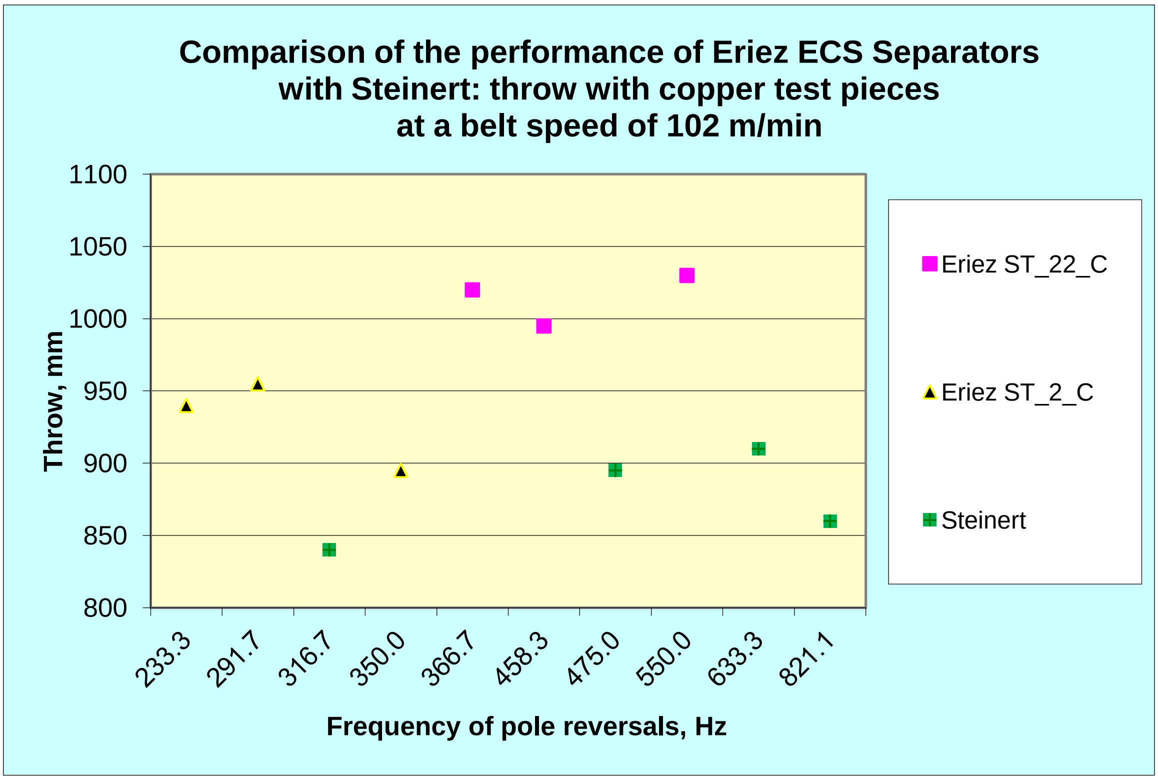

Figure 23 The Gross Throw of Copper Test Pieces at a Belt Speed of 102 m/min

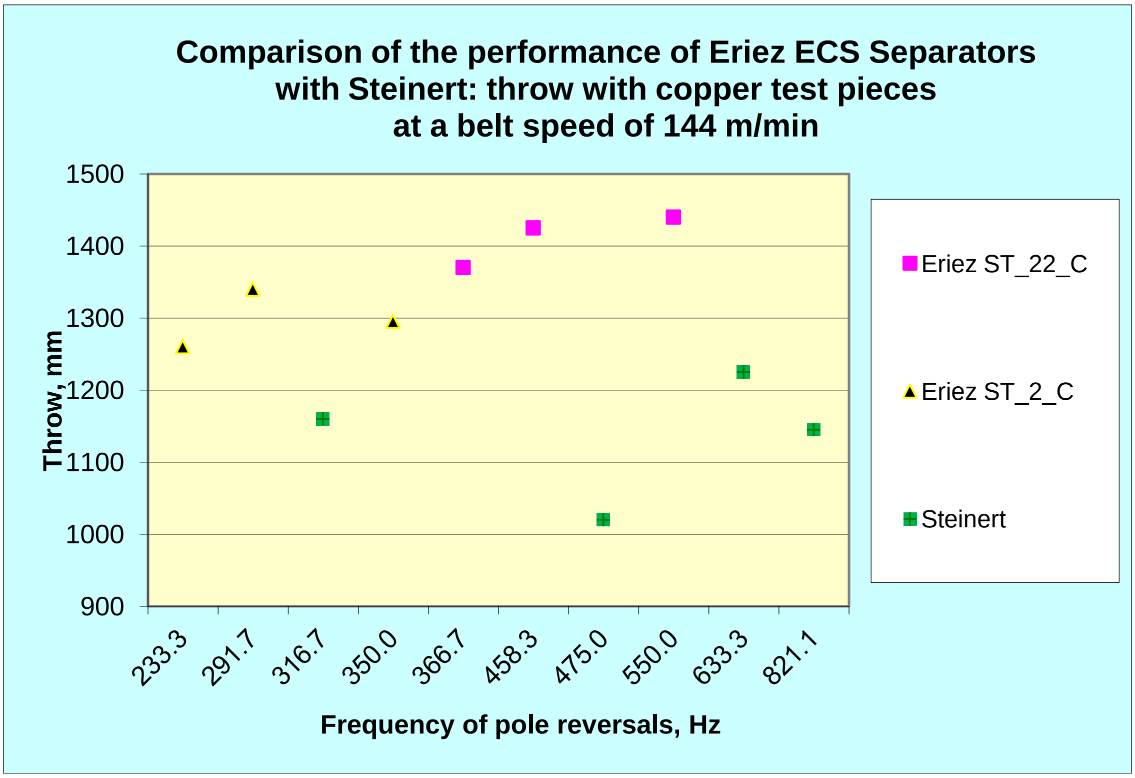

Figure 24 The Gross Throw of Copper Test Pieces at a Belt Speed of 144 m/min

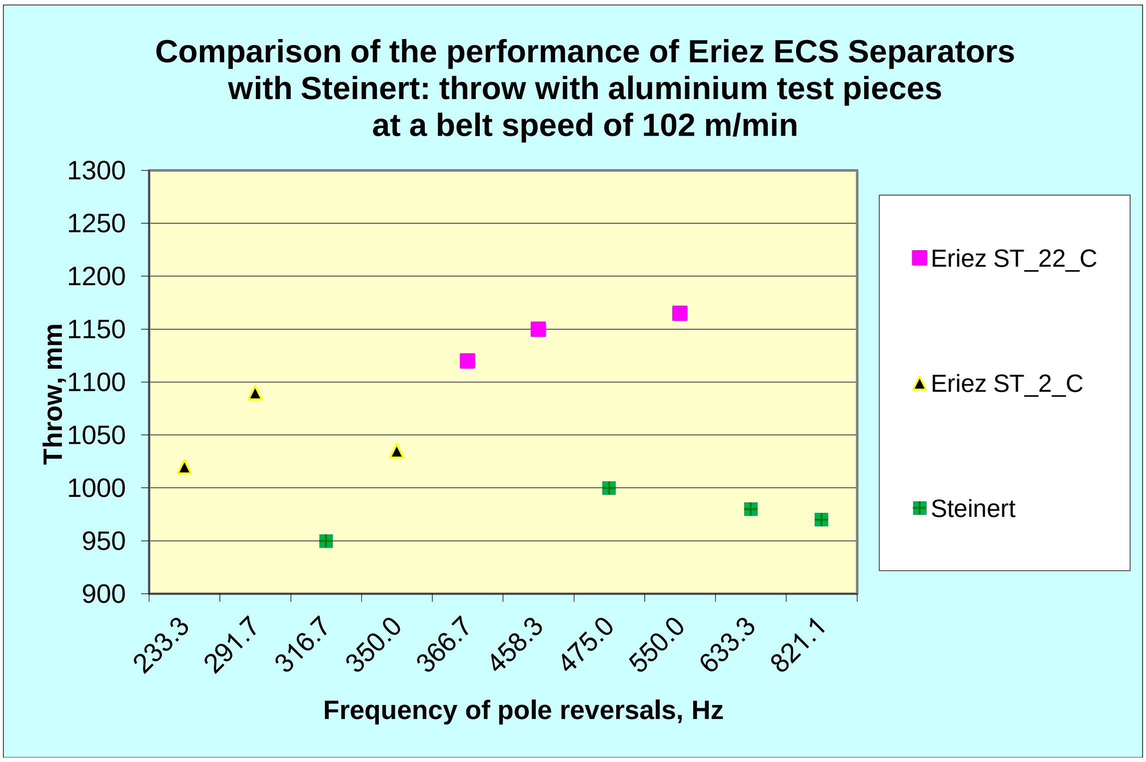

Figure 25 The Gross Throw of Aluminium Test Pieces at a Belt Speed of 102 m/min

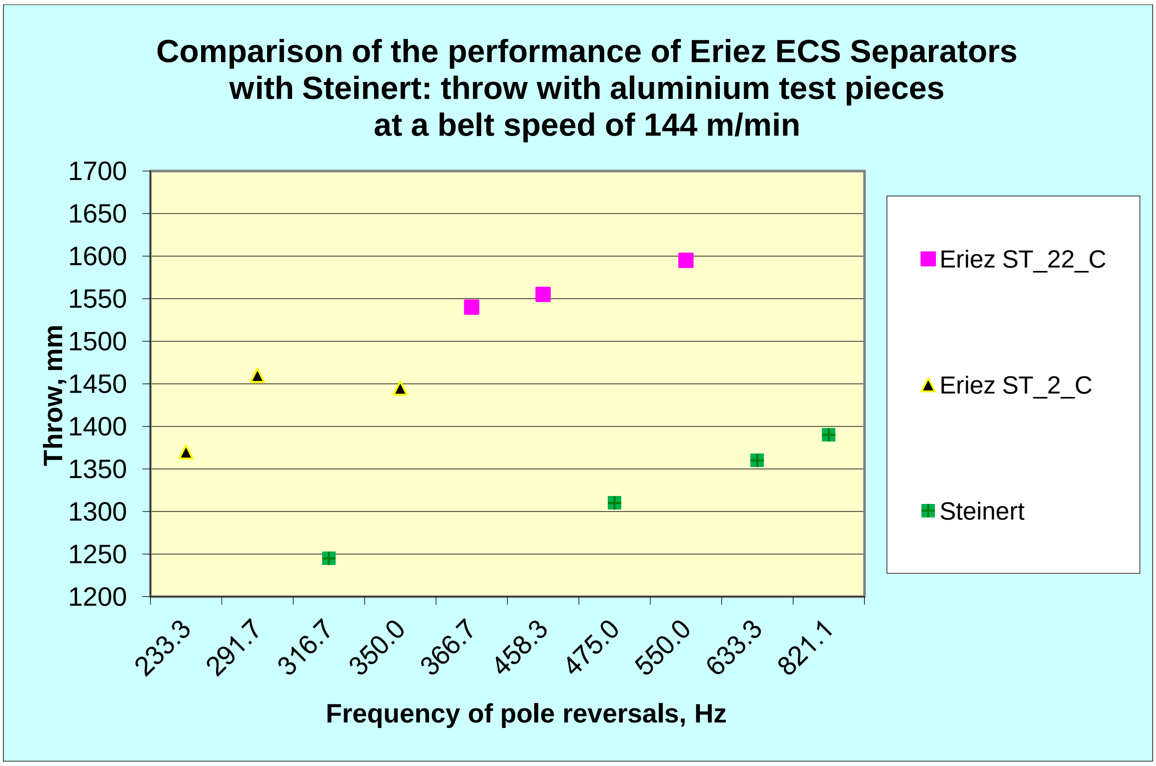

Figure 26 The Gross Throw of Aluminium Test Pieces at a Belt Speed of 144 m/min

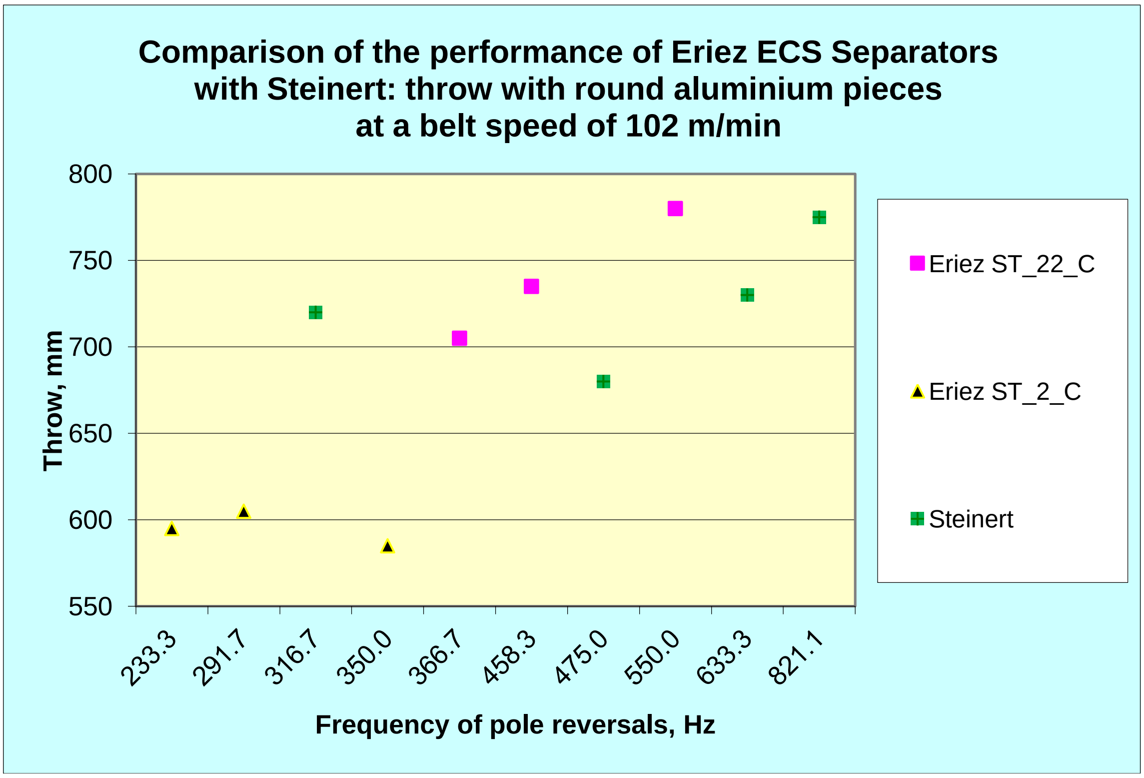

Figure 27 The Gross Throw of Round Aluminium Pieces at a Belt Speed of 102 m/min

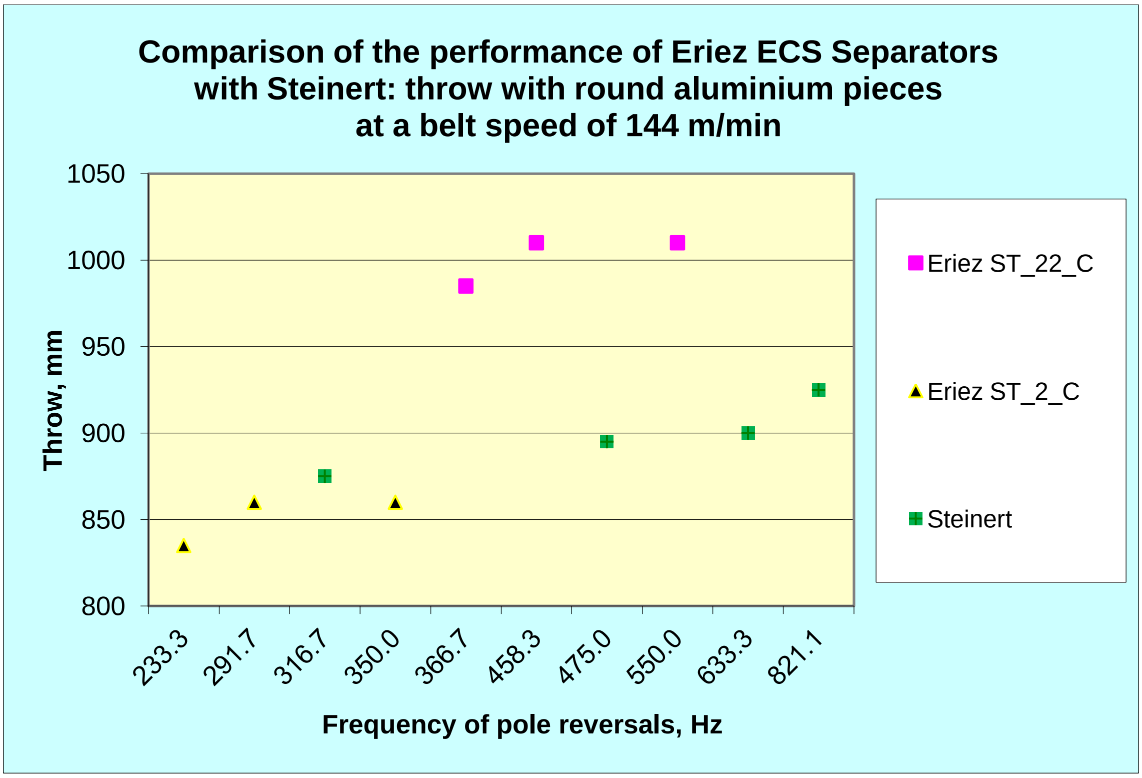

Figure 28 The Gross Throw of Round Aluminium Pieces at a Belt Speed of 144 m/min

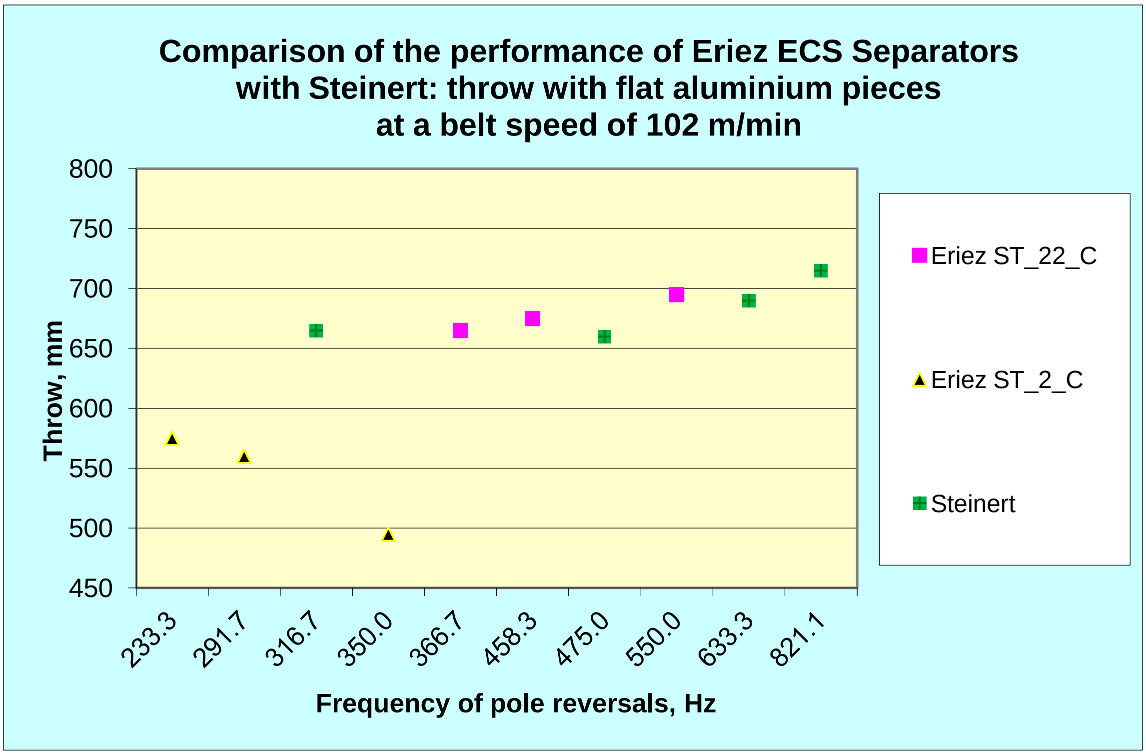

Figure 29 The Gross Throw of Flat Aluminium Pieces at a Belt Speed of 102 m/min

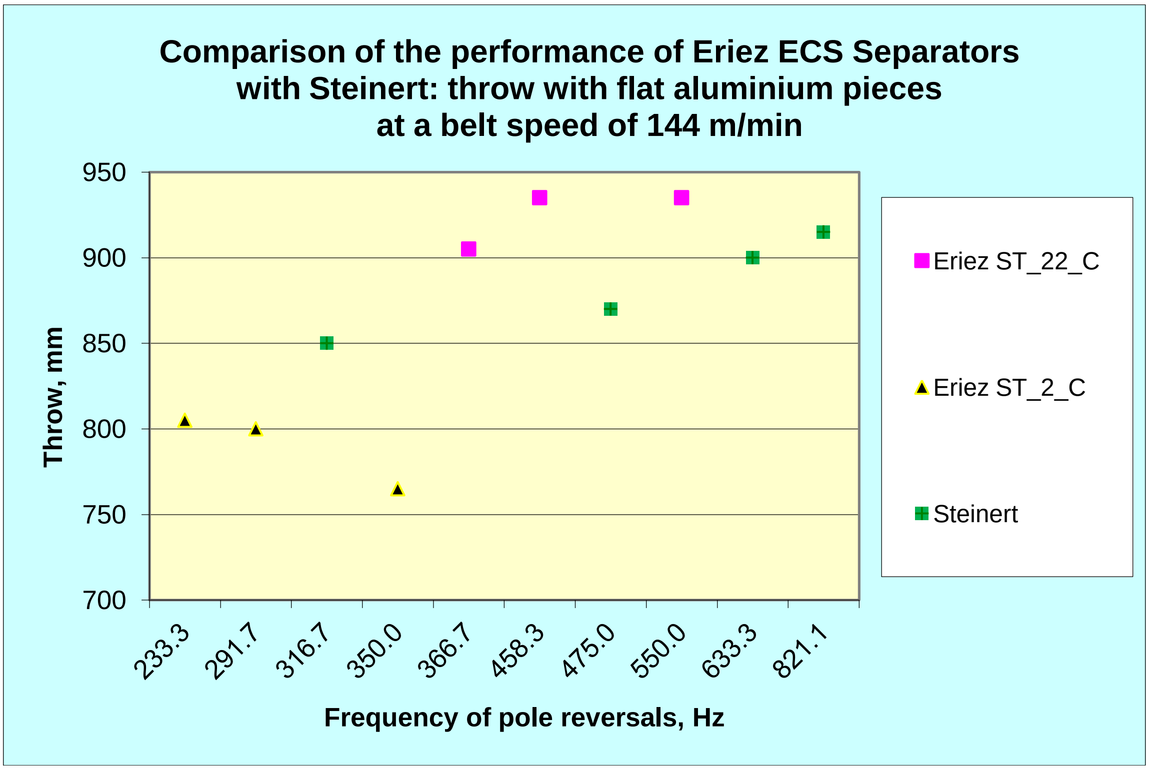

Figure 30 The Gross Throw of Flat Aluminium Pieces at a Belt Speed of 144 m/min

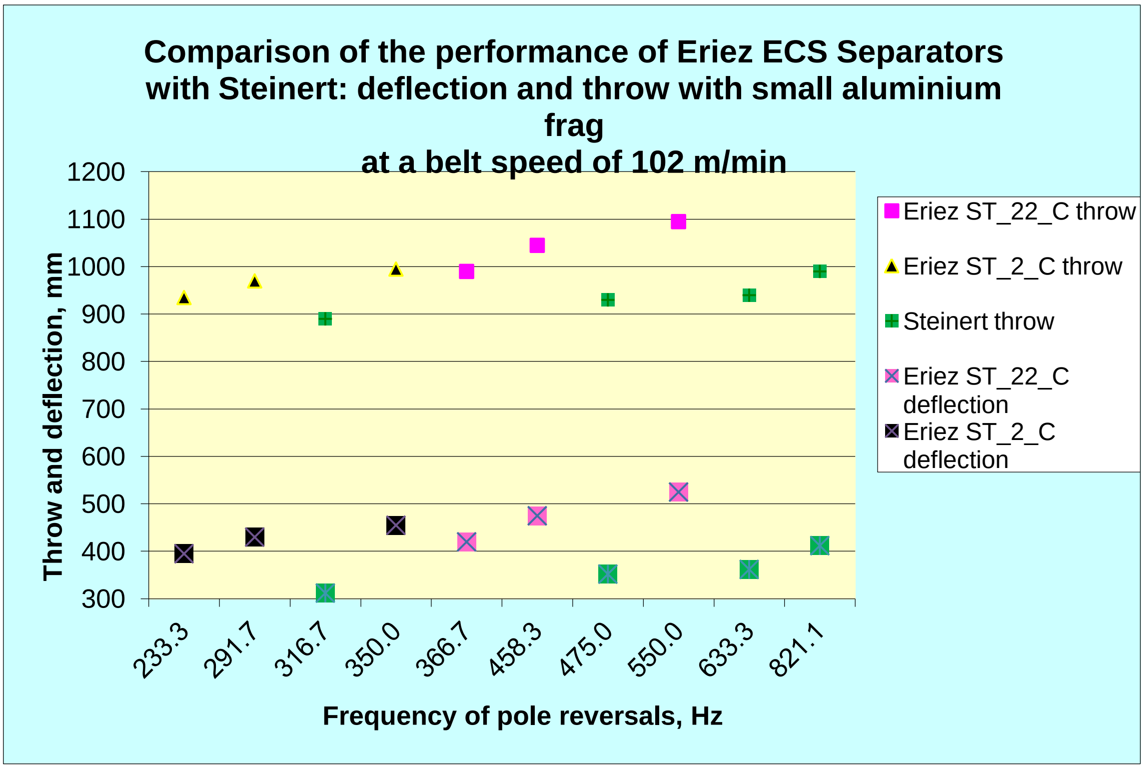

Figure 31 Comparison of the Throw and Nett Deflection of Small Aluminium Frag at a Belt Speed of 102 m/min

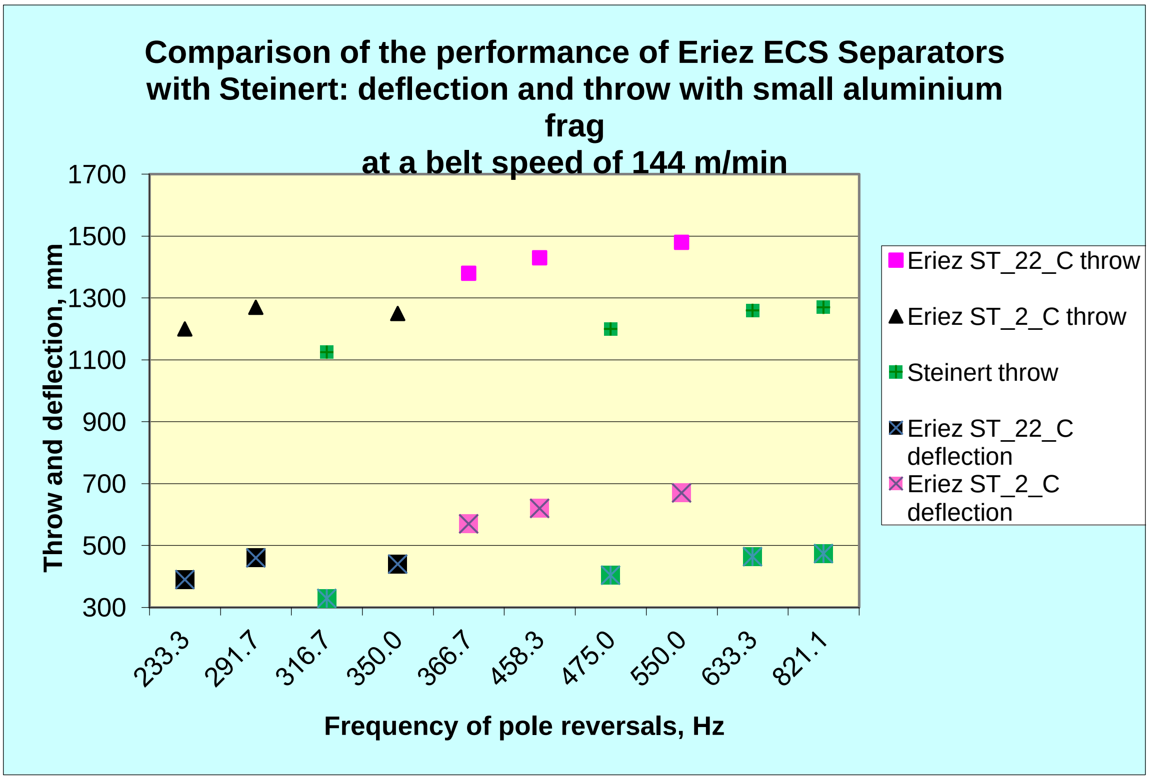

Figure 32 Comparison of the Throw and Nett Deflection of Small Aluminium Frag at a Belt Speed of 144 m/min

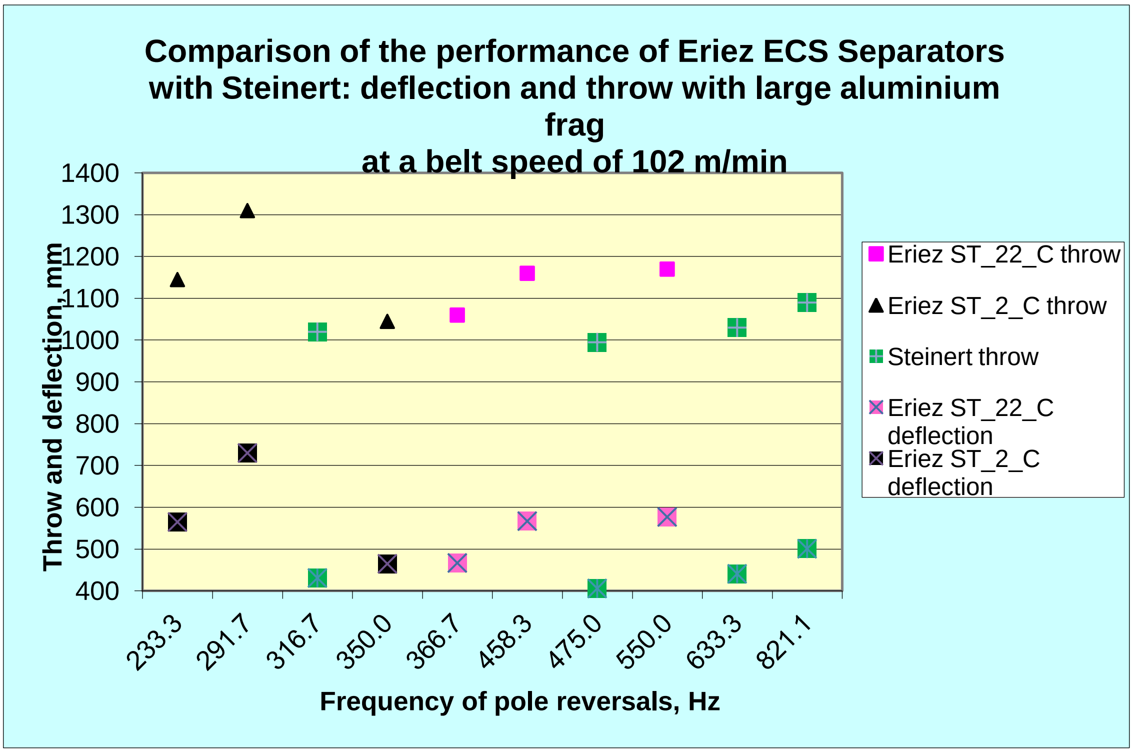

Figure 33 Comparison of the Throw and Nett Deflection of Large Aluminium Frag at a Belt Speed of 102 m/min

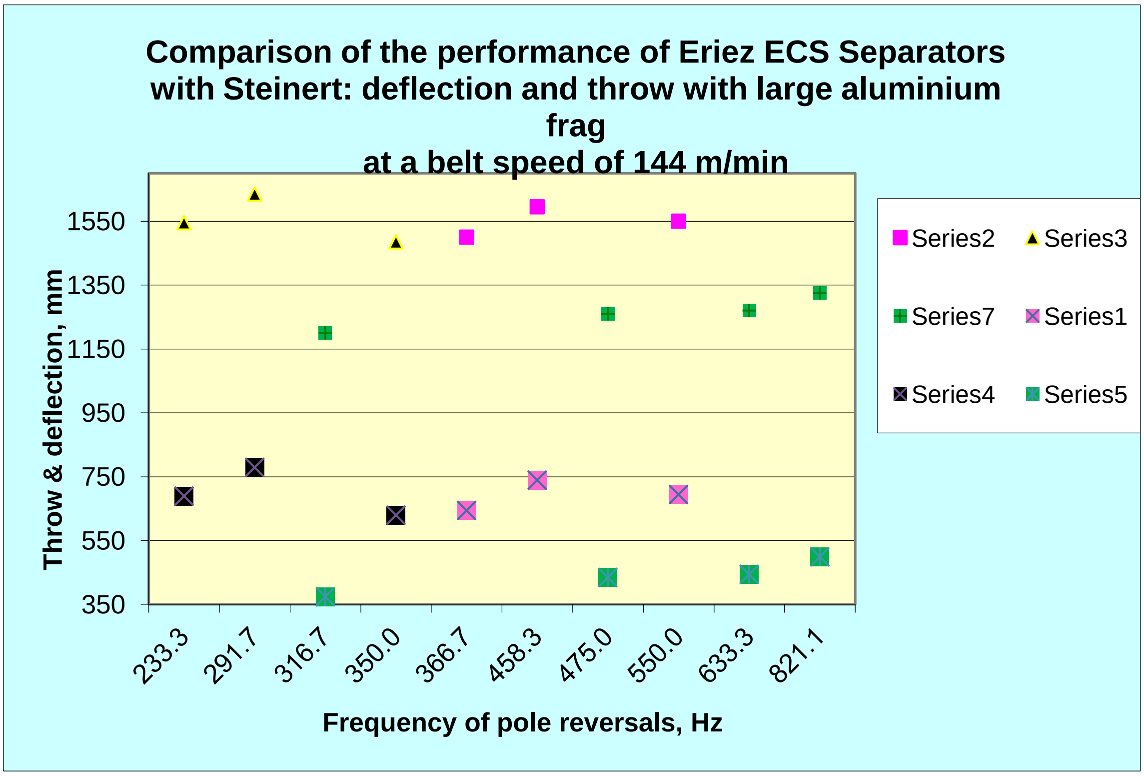

Figure 34 Comparison of the Throw and Nett Deflection of Large Aluminium Frag at a Belt Speed of 144 m/min